Eur. Phys. J. E **8**, 385–401 (2002)
DOI 10.1140/epje/i2002-10025-1

THE EUROPEAN PHYSICAL JOURNAL E
EDP Sciences

Adhesion between an elastic body and a randomly rough hard surface

B.N.J. Persson[a]

IFF, FZ-Jülich, 52425 Jülich, Germany

Received 3 April 2002

Abstract. I have developed a theory of adhesion between an elastic solid and a hard randomly rough substrate. The theory takes into account that partial contact may occur between the solids on all length scales. I present numerical results for the case where the substrate surface is self-affine fractal. When the fractal dimension is close to 2, complete contact typically occurs in the macro-asperity contact areas, while when the fractal dimension is larger than 2.5, the area of (apparent) contact decreases continuously when the magnification is increased. An important result is that even when the surface roughness is so high that no adhesion can be detected in a pull-off experiment, the area of real contact (when adhesion is included) may still be several times larger than when the adhesion is neglected. Since it is the area of real contact which determines the sliding friction force, the adhesion interaction may strongly affect the friction force even when no adhesion can be detected in a pull-off experiment.

PACS. 81.40.Pq Friction, lubrication, and wear – 62.20.-x Mechanical properties of solids

1 Introduction

Even a highly polished surface has surface roughness on many different length scales. When two bodies with nominally flat surfaces are brought into contact, the area of real contact will usually only be a small fraction of the nominal contact area. We can visualize the contact regions as small areas where asperities from one solid are squeezed against asperities of the other solid; depending on the conditions, the asperities may deform elastically or plastically.

How large is the area of *real* contact between a solid block and the substrate? This fundamental question has extremely important practical implications. For example, it determines the contact resistivity and the heat transfer between the solids. It is also of direct importance for sliding friction [1,2], *e.g.*, the rubber friction between a tire and a road surface, and it has a major influence on the adhesive force between two solid blocks in direct contact. I have developed a theory of contact mechanics [3], valid for randomly rough (*e.g.*, self-affine fractal) surfaces, but neglecting adhesion. Adhesion is particularly important for elastically soft solids, *e.g.*, rubber or gelatine, where it may pull the two solids in direct contact over the whole nominal contact area.

The influence of surface roughness on the adhesion between rubber (or any other elastic solid) and a hard substrate has been studied in a classic paper by Fuller and Tabor [4] (see also [5–8]). They found that already a relative small surface roughness can completely remove the adhesion. In order to understand the experimental data they developed a very simple model based on the assumption of surface roughness on a single length scale. In this model the rough surface is modeled by asperities all of the same radius of curvature and with heights following a Gaussian distribution. The overall contact force was obtained by applying the contact theory of Johnson, Kendall and Roberts [9] to each individual asperity. The theory predicts that the pull-off force, expressed as a fraction of the maximum value, depends upon a single parameter, which may be regarded as representing the statistically averaged competition between the compressive forces exerted by the higher asperities trying to prize the surfaces apart and the adhesive forces between the lower asperities trying to hold the surfaces together. We believe that this picture of adhesion developed by Tabor and Fuller would be correct *if* the surfaces had roughness on a single length scale as assumed in their study. However, when roughness occurs on many different length scales, a qualitatively new picture emerges (see below), where, *e.g.*, the adhesion force may even vanish (or at least be strongly reduced), if the rough surface can be described as a self-affine fractal with fractal dimension $D_{\rm f} > 2.5$ (see Sects. 2 and 12). Even for surfaces with roughness on a single length scale, the formalism used by Fuller and Tabor is only valid at "high" surface roughness, where the area of real contact (and the adhesion force) is very small. The theory presented below, on the other hand, is particularly accurate for "small"

[a] e-mail: B.Persson@fz-juelich.de

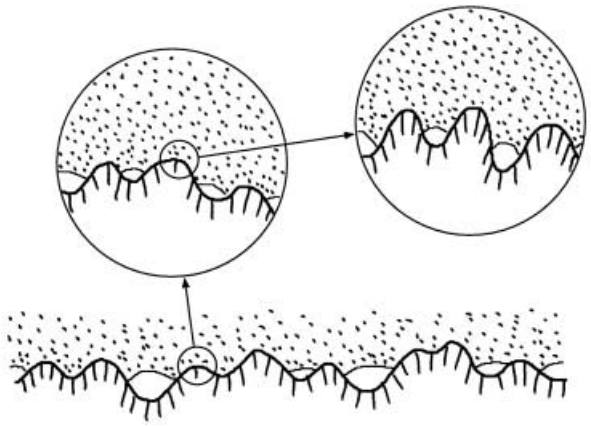

Fig. 1. A rubber block (dotted area) in adhesive contact with a hard rough substrate (dashed area). The substrate has roughness on many different length scales and the rubber makes partial contact with the substrate on all length scales. When a contact area is studied at low magnification it appears as if complete contact occurs, but when the magnification is increased it is observed that in reality only partial contact occurs.

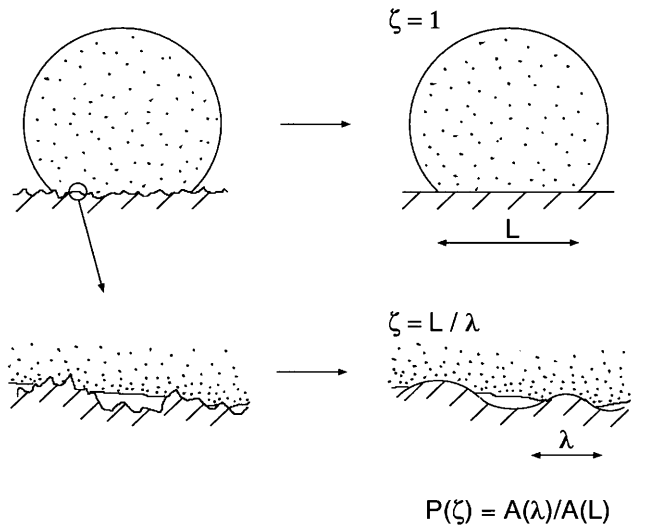

Fig. 2. A rubber ball squeezed against a hard, rough, substrate. Left: The system at two different magnifications. Right: The area of contact $A(\lambda)$ on the length scale λ is defined as the area of real contact, projected on the xy-plane, when the surface roughness on shorter length scales than λ has been removed (*i.e.*, the surface has been "smoothened" on length scales shorter than λ).

surface roughness, where the area of real contact equals the nominal contact area.

In reference [10] we studied adhesion under the assumption that there is complete contact in the nominal contact area. We assumed that the substrate had surface roughness on many different length scales and presented numerical results for the case of self-affine fractal surfaces. In reference [11] we studied adhesion when partial contact occurs, but including "roughness" on a single length scale. In this paper we study adhesion for the most general case, where *partial* contact occurs at the interface on many different length scales, see Figure 1.

We assume randomly rough surfaces, which correspond to asperities of many different sizes and heights. The surface height $h(\mathbf{x})$ is treated as a stochastic variable, characterized by the surface roughness power spectra $C(q)$. This implies asperities of different heights, although for small rms surface roughness, the theory does not depend directly on the surface height probability distribution $P_{\rm h}$. For large rms surface roughness, the surface energy does depend on $P_{\rm h}$, and in this case we have assumed a Gaussian height distribution, but this assumption is not crucial (see App. 2 in Ref. [10]).

The present theory is based on the contact mechanics theory developed in references [3,10]. This theory recognizes that it is very important not to *a priori* exclude any roughness length scale from the analysis. Thus, if $A(\lambda)$ is the (apparent) area of contact on the length scale λ (more accurately, we *define* $A(\lambda)$ to be the real contact area (projected on the xy-plane) if the surface were smooth on all length scales shorter than λ, see Fig. 2), then we study the function $P(\zeta) = A(\lambda)/A(L)$ which is the relative fraction of the rubber surface area where contact occurs on the length scale $\lambda = L/\zeta$ (where $\zeta \geq 1$), with $P(1) = 1$. Here $A(L) = A_0$ denotes the macroscopic (nominal) contact area (L is the diameter of the macroscopic contact area so that $A_0 \approx L^2$).

As an example, Figure 3 shows the dependence of $P(\zeta)$ on the magnification ζ. Results are shown both with and without the adhesion interaction (for details see Sect. 12). Note that without the adhesion, $P(\zeta)$ decreases monotonically with increasing magnification, and, in fact, without a short-distance cut-off, the area of real contact (corresponding to $P(\infty)$) vanishes. When adhesion is included, the (apparent) area of contact equals the area of real contact already at a rather small magnification $\zeta \approx 10$. (This is only the case when the fractal dimension is close to two; in Fig. 3 we have assumed $D_{\rm f} = 2.2$. In Sect. 12 we show that for a large fractal dimension, *e.g.*, 2.6, the area of (apparent) contact decreases continuously with increasing magnification, and, in fact, probably vanishes at infinite magnification (assuming no short-distance cut-off), in accordance with the qualitative discussion in Sect. 2.) Note also that $P(\zeta)$, when the adhesion is included, is always larger than when the adhesion is neglected.

This paper is organized as follows. Section 2 presents a qualitative discussion of the importance of many length scales in adhesion. Section 3 briefly reviews contact mechanics without adhesion. In Section 4 we give expressions for the adhesion and elastic energies, and the effective interfacial energy $\gamma_{\rm eff}$, assuming that complete contact occurs at the interface. Section 5 studies the ball-substrate pull-off force, and points out that the standard JKR expression is also valid for rough surfaces if the longest surface roughness wavelength component is much smaller than the diameter of the nominal contact area. Sections 6 and 7 extend the contact mechanics theory presented in Section 3 to the case of adhesive interaction. In Section 8

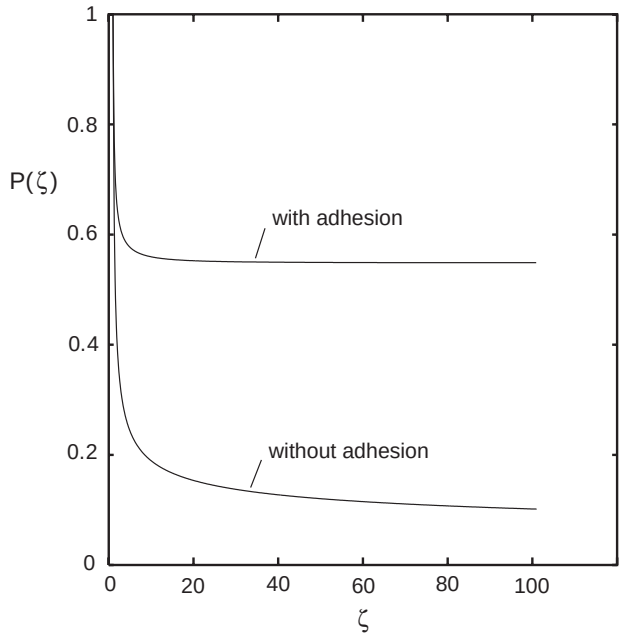

Fig. 3. The dependence of the normalized (apparent) area of contact on the magnification ζ, where $\zeta = 1$ corresponds to the long-distance cut-off length λ_0 in the fractal distribution. Results are shown with and without the adhesion interaction. The applied pressure is $\sigma_0 = 0.05E/(1-\nu^2)$. The fractal exponent $H = 0.8$, $q_0 h_0 = 0.24$ and $\zeta_1 = 100$. For the adhesion curve we used $q_0\delta = 0.1$. See Section 12 for details.

we solve the equations derived in Sections 6 and 7 for the special case of a constant adhesional stress σ_a and show that in the special case of $\sigma_a = 0$ the results of Section 3 are reproduced. In Section 10 we derive an expression for the effective interfacial energy $\gamma_{\rm eff}$, which depends on the function $P(\zeta)$: when $P(\zeta) \equiv 1$ (complete contact on all length scales) the expression for $\gamma_{\rm eff}$ reduces to the result derived in Section 4 for complete contact. Section 11 considers the special case of self-affine fractal surfaces, and in Section 12 we present numerical results for this case. Section 13 compares the theoretical results to experimental data and also suggests a new experiment to test the theoretical results in greater detail. Section 14 summarizes the most important results.

2 Qualitative discussion

Let us estimate the energy necessary in order to deform a rubber block so that the rubber fills out a substrate cavity of height h and width λ. The elastic energy stored in the deformation field in the rubber is given by

$$U_{\rm el} \approx \frac{1}{2}\int {\rm d}^3x\ \sigma\epsilon\,,$$

where the stress $\sigma \approx E\epsilon$, where E is the elastic modulus. The deformation field is mainly localized to a volume $\sim \lambda^3$ (see Fig. 4) where the strain $\epsilon \approx h/\lambda$. Thus we get $U_{\rm el} \approx \lambda^3 E(h/\lambda)^2 = E\lambda h^2$.

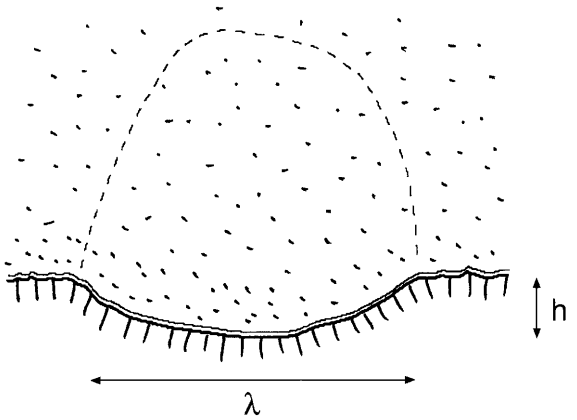

Fig. 4. Rubber (dotted area) filling out a substrate cavity. The deformation (elastic) energy in the rubber is mainly localized to a volume element of size λ^3 (bounded by the dashed line), where the strain is of order $\sim h/\lambda$.

Let us now consider the role of the rubber-substrate adhesion interaction. As shown above, when the rubber deforms and fills out a surface cavity of the substrate, an elastic energy $U_{\rm el} \approx E\lambda h^2$ will be stored in the rubber. Now, if this elastic energy is smaller than the gain in adhesion energy $U_{\rm ad} \approx -\Delta\gamma\lambda^2$, where $\Delta\gamma = \gamma_1 + \gamma_2 - \gamma_{12}$ is the change of surface free energy (per unit area) upon contact due to the rubber-substrate interaction (which usually is mainly of the van der Waals type), then (even in the absence of an external load $F_{\rm N}$) the rubber will deform *spontaneously* to fill out the substrate cavities. The condition $U_{\rm el} = -U_{\rm ad}$ gives $h/\lambda \approx (\Delta\gamma/E\lambda)^{1/2}$. For example, for very rough surfaces with $h/\lambda \approx 1$, and with parameters typical for rubber $E = 1$ MPa and $\Delta\gamma = 3$ meV/Å^2, the adhesion interaction will be able to deform the rubber and completely fill out the cavities if $\lambda < 0.1$ μm. For very smooth surfaces $h/\lambda \sim 0.01$ or smaller, so that the rubber will be able to follow the surface roughness profile up to the length scale $\lambda \sim 1$ mm or longer.

The argument given above shows that for elastic solids with surface roughness on a *single length scale* λ, the competition between adhesion and elastic deformation is characterized by the parameter $\theta = Eh^2/\lambda\Delta\gamma$, where h is the amplitude of the surface roughness. The parameter θ is the ratio between the elastic energy and the surface energy stored at the interface, assuming that complete contact occurs. When $\theta \gg 1$ only partial contact occurs, where the elastic solids make contact only close to the top of the highest asperities, while complete contact occurs when $\theta \ll 1$.

Surfaces or real solids have roughness on a wide distribution of length scales. Assume, for example, a self-affine fractal surface. In this case the statistical properties of the surface are invariant under the transformation

$$\mathbf{x} \to \mathbf{x}\,\zeta, \qquad z \to z\,\zeta^H\,,$$

where $\mathbf{x} = (x, y)$ is the 2D position vector in the surface plane, and where $0 < H < 1$. This implies that if h_a is the amplitude of the surface roughness on the length scale

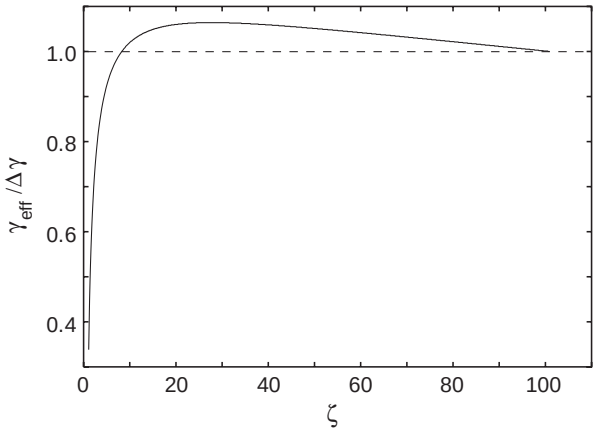

Fig. 5. The dependence of the effective interfacial energy on the magnification ζ, where $\zeta = 1$ corresponds to the long-distance cut-off length λ_0 in the fractal distribution. The applied pressure is $\sigma_0 = 0.05E/(1-\nu^2)$. The fractal exponent $H = 0.8$, $q_0 h_0 = 0.24$, $q_0\delta = 0.1$ and $\zeta_1 = 100$. See Section 12 for details.

$\lambda_{\rm a}$, then the amplitude h of the surface roughness on the length scale λ will be of order

$$h \approx h_{\rm a}\ (\lambda/\lambda_{\rm a})^H\,.$$

Thus we get

$$\theta_{\rm a} = \theta(\lambda_{\rm a}/\lambda)^{2H-1}\,,$$

where $\theta_{\rm a} = Eh_{\rm a}^2/\lambda_{\rm a}\Delta\gamma$. Hence, when we study the system on shorter and shorter length scale $\lambda_{\rm a} < \lambda$, $\theta_{\rm a}$ will decrease or increase depending on if $H > 1/2$ and $H < 1/2$, respectively. In the former case, if $\theta < 1$ the adhesion will be important on any length scale $\lambda_{\rm a} < \lambda$. In particular, if λ is the long-distance cut-off length λ_0 in the self-affine fractal distribution, then *complete contact will occur at the interface*. In the latter case, even if $\theta < 1$ so that the adhesion may seem important on the length scale λ, at short enough length scale $\theta_{\rm a} > 1$. Thus, without a short-distance cut-off, the adhesion and the area of real contact will vanish. In reality, a finite short-distance cut-off will always occur, but this case requires a more detailed study.

The present problem, involving many length scales, will be studied below by a renormalization group type of approach, where during the process of eliminating short-wavelength roughness components, the effective interfacial energy $\gamma_{\rm eff}(\zeta)$ and the normalized (apparent) area of contact $P(\zeta)$ depend on the length scale $\lambda = L/\zeta$ of observation. For example, for the case considered in Figure 3 (with adhesion), the effective interfacial energy is shown in Figure 5 as a function of the magnification ζ. Note that at short length scale (large ζ) $\gamma_{\rm eff}(\zeta)$ increases with decreasing magnification. This effect results from the increase in the surface area because of the surface roughness. However, at long length scale $\gamma_{\rm eff}(\zeta)$ decreases below $\Delta\gamma$. This effect results from the contribution to the interfacial free energy from the elastic deformation energy induced in the rubber by the substrate surface roughness (see Sects. 4 and 12). Note also that $\gamma_{\rm eff}$ at the shortest length scale (which in the present case corresponds to the magnification $\zeta = 100$) equals the "bare" value $\Delta\gamma$ as it should. In the language of the renormalization group (RG) theory, we can consider the equations which determine $\gamma_{\rm eff}(\zeta)$ and $P(\zeta)$ as the RG-flow equations.

3 Contact mechanics without adhesion

Let us briefly review the theory presented in reference [3]. From contact mechanics (see, *e.g.*, Ref. [12]) it is known that in the frictionless contact of elastic solids with rough surfaces, the contact stresses depend only upon the shape of the gap between them before loading. Thus, without loss of generality, the actual system may then be replaced by a flat elastic surface (elastic modulus E and Poisson ratio ν, related to the original quantities *via* $(1-\nu^2)/E = (1-\nu_1^2)/E_1 + (1-\nu_2^2)/E_2$) in contact with a rigid body having a surface roughness profile which results in the same undeformed gap between the surfaces.

Consider the system at the length scale $\lambda = L/\zeta$, where L is of order of the diameter of the nominal contact area. We define $q_L = 2\pi/L$ and write $q = q_L\zeta$. Let $P(\sigma,\zeta)$ denote the stress distribution in the contact areas under the magnification ζ. Here $\sigma = \sigma_{zz}$ is the surface stress component in the z-direction. The function $P(\sigma,\zeta)$ satisfies the differential equation (see Ref. [3]):

$$\frac{\partial P}{\partial \zeta} = f(\zeta)\frac{\partial^2 P}{\partial \sigma^2}\,, \tag{1}$$

where $f(\zeta) = G'(\zeta)\sigma_0^2$, where $G'(\zeta)$ denotes the ζ-derivative of the function

$$G(\zeta) = \frac{\pi}{4}\left[\frac{E}{(1-\nu^2)\sigma_0}\right]^2 \int_{q_L}^{\zeta q_L} {\rm d}q\ q^3 C(q). \tag{2}$$

The surface roughness power spectra

$$C(q) = \frac{1}{(2\pi)^2}\int {\rm d}^2x\ \langle h(\mathbf{x})h(\mathbf{0})\rangle e^{-i\mathbf{q}\cdot\mathbf{x}},$$

where $z = h(\mathbf{x})$ is the height of the surface above a flat reference plane (chosen so that $\langle h\rangle = 0$), and $\langle ...\rangle$ stands for ensemble average. For many surfaces $C(q)$ has the form shown in Figure 6.

Let us write

$$P(\sigma,1) = P_0(\sigma).$$

If we assume a constant pressure in the nominal contact area, then $P_0(\sigma) = \delta(\sigma - \sigma_0)$.

Equation (1) is a diffusion type of equation, where time is replaced by the magnification ζ, and the spatial coordinate with the stress σ (and where the "diffusion constant" depends on ζ). Hence, when we study $P(\sigma,\zeta)$ on shorter and shorter length scales (corresponding to increasing ζ), the $P(\sigma,\zeta)$ function will become broader and broader in σ-space. (The physical origin of this effect is clear: the block-substrate asperity contact areas will give rise to a wide distribution of local contact stresses. As the system

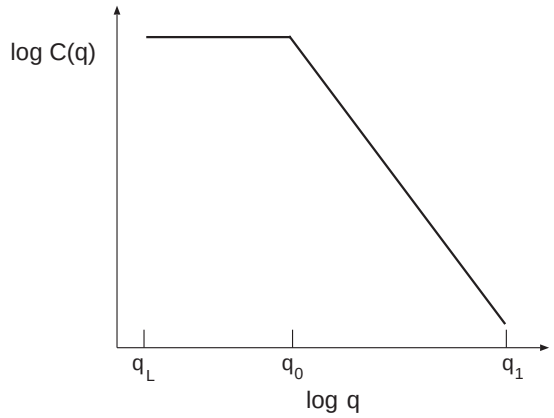

Fig. 6. Qualitative form of the surface roughness power spectra observed for many real surfaces. q_1 is the short-distance cut-off wave vector which cannot be larger than $2\pi/a$, where a is the lattice constant. q_0 is the crossover wave vector, from a power law $\sim q^{-2(H+1)}$ for $q > q_0$ to a constant for $q < q_0$. For engineering surfaces one typically has $q_0 \sim 1/(10\ \mu\text{m})$, and for road surfaces $q_0 \sim 1/(1\ \text{cm})$. The lateral size L of the nominal contact area determines the long-distance (small-wave vector) cut-off $q_L \approx 2\pi/L$. For surfaces prepared by fracture one typically has $q_0 = q_L$.

is studied at higher and higher magnification, a wider distribution of asperity sizes are observed and the stress distribution will become wider and wider.) We can take into account that detachment actually will occur when the local stress reaches $\sigma = 0$ (we assume no adhesion) *via* the boundary condition:

$$P(0, \zeta) = 0.$$

We assume that only elastic deformation occurs (*i.e.*, the yield stress $\sigma_Y \to \infty$). In this case (see Ref. [3] and Sect. 7):

$$P(\zeta) = \int_0^\infty \mathrm{d}\sigma P(\sigma, \zeta)\,.$$

It is straightforward to solve (1) with the boundary conditions $P(0, \zeta) = 0$ and $P(\sigma_Y, \zeta) = 0$ by expanding $P(\sigma, \zeta) = \sum_n A_n(\zeta)\, \sin(n\pi\sigma/\sigma_Y)$. In the elastic limit $\sigma_Y \to \infty$ we get

$$P(\zeta) = \frac{2}{\pi} \int_0^\infty \mathrm{d}x\ \frac{\sin x}{x}\ \exp\left[-x^2 G(\zeta)\right]\,. \qquad (3)$$

An alternative approach is to put $\sigma_Y = \infty$ from the beginning, and Laplace-transform the σ-dependence in equation (1). In the present case this approach is more complicated, but later when we include adhesion (see Sect. 6) only this approach is possible.

We consider now the limit $\sigma_0 \ll E$, which is satisfied in most applications. In this case, for most ζ-values of interest, $G(\zeta) \gg 1$, so that only $x \ll 1$ will contribute to the integral in (3), and we can approximate $\sin x \approx x$ and

$$P(\zeta) \approx \frac{2}{\pi} \int_0^\infty \mathrm{d}x\, \exp\left[-x^2 G(\zeta)\right] = \left[\pi G(\zeta)\right]^{-1/2}. \qquad (4)$$

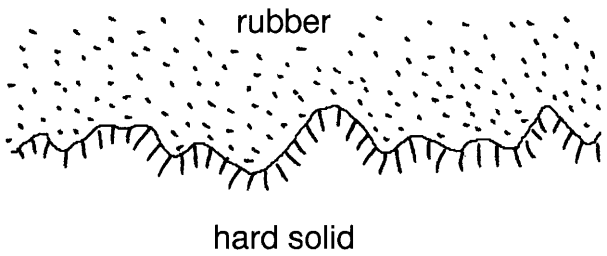

Fig. 7. The adhesion interaction pulls the rubber into complete contact with the rough substrate surface.

Thus, within this approximation, using (2) and (4) we get $P(\zeta) \propto \sigma_0$ so that the area of real contact is proportional to the load.

4 Interfacial elastic and adhesion energies for rough surfaces

Assume that a flat rubber surface is in contact with the rough surface of a hard solid. Assume that because of the rubber-substrate adhesion interaction, the rubber deforms elastically and makes contact with the substrate everywhere, see Figure 7.

Let us calculate the difference in free energy between the rubber block in contact with the substrate and the non-contact case. Let $z = h(\mathbf{x})$ denote the height of the rough surface above a flat reference plane (chosen so that $\langle h \rangle = 0$). Assume first that the rubber is in direct contact with the substrate over the whole nominal contact area. The surface adhesion energy is assumed proportional to the contact area so that

$$U_{\rm ad} = -\Delta\gamma \int \mathrm{d}^2x\ \left(1 + [\nabla h(\mathbf{x})]^2\right)^{1/2}, \qquad (5a)$$

where $\Delta\gamma = \gamma_1 + \gamma_2 - \gamma_{12}$. In reference [10] we have derived a general expression for $U_{\rm ad}$ which is valid for arbitrary magnitude of $|\nabla h|$:

$$U_{\rm ad} = -\Delta\gamma A_0 \int_0^\infty \mathrm{d}x \left(1 + x\xi^2\right)^{1/2} e^{-x}\,, \qquad (5b)$$

where

$$\xi^2 = \int \mathrm{d}^2q\ q^2 C(q)\,.$$

When $\xi \ll 1$, (5b) reduces to

$$U_{\rm ad} \approx -\Delta\gamma A_0 \left[1 + \frac{1}{2}\int \mathrm{d}^2q\ q^2 C(q)\right]. \qquad (5c)$$

This approximation corresponding to expanding the integrand in (5a) to first order in $(\nabla h)^2$.

Next, let us consider the elastic energy stored in the deformation field in the vicinity of the interface. If we assume that complete contact occurs between the solids, then, as shown in reference [10],

$$U_{\rm el} \approx \frac{A_0 E}{4(1-\nu^2)} \int \mathrm{d}^2q\ qC(q)\,, \qquad (6)$$

where E is the elastic modulus and ν the Poisson ratio.

The change in the free energy when the rubber block moves in contact with the substrate is given by the sum of (5) and (6):

$$U_{\rm el} + U_{\rm ad} = -\gamma_{\rm eff} A_0 \,,$$

where

$$\frac{\gamma_{\rm eff}}{\Delta\gamma} = \int_0^\infty {\rm d}x \left(1+x\xi^2\right)^{1/2} e^{-x} - \frac{2\pi}{\delta}\int_{q_0}^{q_1} {\rm d}q\; q^2 C(q) \qquad (7)$$

or, when $\xi \ll 1$,

$$\frac{\gamma_{\rm eff}}{\Delta\gamma} = 1 + \pi\int_{q_0}^{q_1} {\rm d}q\; q^3 C(q) - \frac{2\pi}{\delta}\int_{q_0}^{q_1} {\rm d}q\; q^2 C(q)\,. \qquad (8)$$

In the equations above we have introduced the *adhesion length*

$$\delta = 4(1-\nu^2)\Delta\gamma/E\,. \qquad (9)$$

The theory above is valid for surfaces with arbitrary random roughness, but will now be applied to self-affine fractal surfaces. It has been found that many "natural" surfaces, *e.g.*, surfaces of many materials generated by fracture, can be approximately described as self-affine surfaces over a rather wide roughness size region. A self-affine fractal surface has the property that if we make a scale change that is appropriately different along the two directions, parallel and perpendicular, then the surface does not change its morphology [13]. Recent studies have shown that even asphalt road tracks (of interest for rubber friction) are (approximately) self-affine fractal, with an upper cut-off length $\lambda_0 = 2\pi/q_0$ of order ~ 1 cm [14]. We take [13,15] $C(q) = 0$ for $q < q_0$, while for $q > q_0$:

$$C(q) = \frac{H}{2\pi}\left(\frac{h_0}{q_0}\right)^2 \left(\frac{q}{q_0}\right)^{-2(H+1)}\,, \qquad (10)$$

where $H = 3-D_{\rm f}$ (where the fractal dimension $2 < D_{\rm f} < 3$), and where q_0 is the lower cut-off wave vector, and h_0 is determined by the rms roughness amplitude, $\langle h^2\rangle = h_0^2/2$. We note that $C(q)$ can be measured directly, using many different methods, *e.g.*, using stylus instruments or optical instruments [16].

Substituting (10) in (8) gives

$$\frac{\gamma_{\rm eff}}{\Delta\gamma} = 1 + (q_0 h_0)^2\left(\frac{1}{2}g(H) - \frac{1}{q_0\delta}f(H)\right)$$

or

$$\frac{\gamma_{\rm eff}}{\Delta\gamma} = 1 + \frac{1}{2}(q_0 h_0)^2 g(H)\left(1 - \frac{\alpha(H)}{q_0\delta}\right)\,, \qquad (11)$$

where $\alpha(H) = 2f(H)/g(H)$ is the *roughness parameter*, and where

$$f(H) = \frac{H}{1-2H}\left(\zeta_1^{1-2H} - 1\right)\,,$$

$$g(H) = \frac{H}{2(1-H)}\left(\zeta_1^{2(1-H)} - 1\right)\,,$$

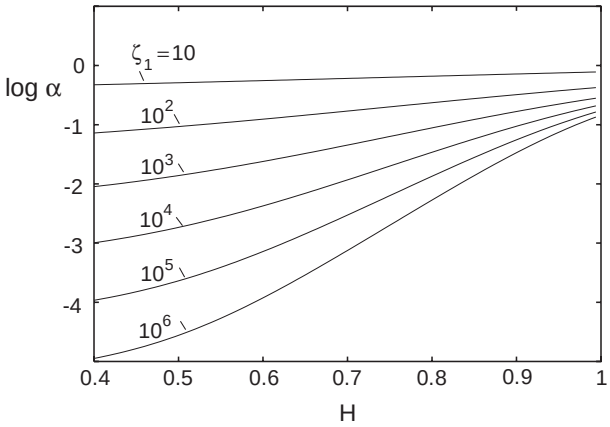

Fig. 8. The logarithm (with 10 as basis) of the roughness parameter α as a function of the roughness exponent H and for different ranges of roughness, $\zeta_1 = q_1/q_0$.

where $\zeta_1 = q_1/q_0$. In Figure 8 we show $\alpha(H)$ as a function of H.

Note that if the condition $\alpha < q_0\delta$ is satisfied, the adhesion force (for small enough h_0) will increase with increasing amplitude h_0 of the surface roughness. We may define a critical elasticity $E_{\rm c}$ such that if $E < E_{\rm c}$, $\Delta\gamma_{\rm eff}$ increases with increasing h_0 (for small h_0), while it decreases if $E > E_{\rm c}$. $E_{\rm c}$ is determined by the condition $\alpha(H) = q_0\delta$ which gives

$$E_{\rm c} = 4(1-\nu^2)\Delta\gamma q_0/\alpha(H)\,. \qquad (12)$$

This expression for $E_{\rm c}$ depends on the nature of the surface roughness *via* the cut-off wave vector q_0 and the fractal exponent $H = 3-D_{\rm f}$. These quantities can be obtained from measurements of the surface roughness power spectra $C(q)$. Such measurements have not been performed for any of the system for which the dependence of the adhesion on the roughness amplitude h_0 has been studied. However, measurements [16] of $C(q)$ for similar surfaces as those used in the adhesion experiments have shown that typically $H \approx 0.8$ and $\lambda_0 = 2\pi/q_0 \approx 100$ μm. For $H \approx 0.8$, Figure 8 gives for typical ζ_1, $\alpha(H) \sim 0.01$ and with the measured (for rubber in contact with most hard solids) $\Delta\gamma \approx 3$ meV/Å^2 we get $E_{\rm c} \approx 1$ MPa. This is in very good agreement with experimental observations. Thus, Briggs and Briscoe [5] observed a strong roughness-induced increase in the pull-off force for rubber with the elastic modulus $E = 0.06$ MPa, but a negligible increase when $E = 0.5$ MPa. Similarly, Fuller and Roberts [6] observed an increase in the pull-off force for rubbers with $E = 0.4$, 0.14 and 0.07 MPa, but a continuous decrease for rubbers with $E = 1.5$ and 3.2 MPa. It would be extremely interesting to perform a detailed test of the theory for surfaces for which the surface roughness power spectra $C(q)$ have been measured (see Sect. 13).

Note that for elastically very soft solids adhesion will always be important in practical applications. For example, for gelatine we have $E \approx 10^4$ Pa and with $\Delta\gamma \approx 3$ meV/Å^2 we get $\delta \approx 10$ μm. Since typically $q_0 = 2\pi/\lambda_0 \sim (10\ \mu{\rm m})^{-1}$ and $\alpha(H) \ll 1$, we expect $\Delta\gamma_{\rm eff} > \Delta\gamma$ for small

surface roughness. Thus, for an (elastically) very soft solid the adhesion force may increase upon roughening the substrate surface. As pointed out above, this effect has been observed experimentally for rubber in contact with a hard, rough substrate [5,6], and the present theory explains under exactly what conditions that will occur.

The result (11) is based on an expansion of the surface area to second order in h_0. For "large" surface roughness this approximation breaks down and it is clear that for large h_0, the area of contact will be proportional to h_0. Since the elastic energy is proportional to h_0^2, it follows that for large enough rms amplitude of the surface roughness, the elastic term will cancel the adhesion term and no adhesion will be observed. Thus, even if $\alpha(H) < q_0\delta$ so that the adhesion force initially increases upon increasing h_0 from zero, at large enough h_0 the adhesion force must decrease. This is observed in the numerical results presented in reference [10] and also below in Section 12.

For most (clean) solids surfaces, $\Delta\gamma \approx Ea$, where a is an atomic distance (of order ~ 1 Å) and E the elastic modulus. (This relation holds only if the elastic modulus E is due to the stretching of atomic bonds, and is not valid for, *e.g.*, rubber where E has an entropic origin.) Thus, $\delta \sim a \sim 1$ Å so that typically $q_0\delta \sim 10^{-5}$, and the condition $\alpha(H) \gg q_0\delta$ will be satisfied in most cases of interest. That is, the (repulsive) energy stored in the elastic deformation field in the solids at the interface largely overcomes the adhesion energy, and adhesion will be negligible. This explains the *adhesion paradox*, namely why adhesion usually is not observed when macroscopic solids are separated.

In Section 12 we will present numerical results illustrating adhesion when $H = 0.4$ and 0.8 and for $\zeta_1 = 100$ and 1000. For these cases we have

$$\alpha(0.4) = 0.073, \quad \alpha(0.8) = 0.235 \quad \text{for} \quad \zeta_1 = 100\,,$$

$$\alpha(0.4) = 0.009, \quad \alpha(0.8) = 0.088 \quad \text{for} \quad \zeta_1 = 1000\,.$$

5 Pull-off force

Consider a rubber ball (radius R_0) in adhesive contact with a perfectly smooth and hard substrate. The elastic deformation of the rubber can be determined by minimizing the total energy which is the sum of the (positive) elastic energy stored in the deformation field in the rubber ball, and the (negative) binding energy between the ball and the substrate at the contact interface. The free energy minimization gives the pull-off force

$$F_c = (3\pi/2)R_0\Delta\gamma\,. \tag{13}$$

This result was first derived by Sperling [17] and (independently) by Johnson, Kendall and Roberts [9]. Kendall has reported similar results for other geometries of interest [18].

Consider now the same problems as above, but assume that the substrate surface has roughness described by the function $z = h(\mathbf{x})$. We now study how the adhesion force is reduced from the ideal value (13) as the amplitude of the surface roughness is increased. Let us first assume that the adhesive interaction is so strong that the elastic solid is in contact with the substrate everywhere, and that the width L of the nominal contact area is much larger than the long-distance cut-off (or roll-off) length λ_0 of the surface roughness power spectra. In this case we can still use the result (13), but with $\Delta\gamma$ replaced by $\Delta\gamma_{\rm eff}$ as given by (7). This approach can also be used when partial contact occurs at the interface, which will always be the case at large enough surface roughness, and below we consider this case in detail.

We note that accounting for the surface roughness by replacing $\Delta\gamma$ with $\gamma_{\rm eff}$ is formally exact, at least as long as $\lambda_0 \ll L$. Intuitively, one can understand this by noticing that even a "flat" substrate is in reality corrugated (atomic corrugation, steps and so on), but this effect is already included in the definition of $\Delta\gamma$. The basic physical assumption is a wide separation of length scales: the lateral size L of the macroscopic contact area is assumed to be much larger than the amplitude and the wavelength of the surface roughness, so that when solving for the elastic deformation of the rubber ball on the length scale L, one does not need to account directly for the small-sized surface roughness (but the latter enters indirectly *via* the effective surface energy $\gamma_{\rm eff}$), while when calculating the deformations of the rubber ball on the length scale λ_0 or shorter, one may neglect the elastic deformations of the rubber ball on the length scale L.

Note that the elastic forces (induced by the surface roughness) and the surface forces at the interface always balance (independent of the amplitude of the surface roughness) in the sense that the total force which acts on a small rubber volume element at the interface vanishes. The (macroscopic) effective surface energy, $\gamma_{\rm eff}(1)$, however, will only vanish when the surface roughness amplitude is big enough. What happens then is that the elastic energy stored at the interface is just large enough to break the adhesive bond between the two surfaces; during the pull-off this energy is given back and therefore no adhesion is observed during the pull-off.

In the JKR theory, for an elastic sphere in contact with a perfectly flat substrate, the adhesion and elastic forces also balance in the sense described above. However, at zero applied external force, the elastic energy stored in the ball is smaller than the surface energy due to the rubber-substrate interaction (by a factor 2/5), and a finite amount of energy must therefore be used to remove the ball from the substrate, resulting in a non-zero pull-off force.

6 Stress probability distribution

The discussion in Section 4 assumed complete contact at the interface. We will now generalize the theory to the case of partial contact. The theory below is based on the contact mechanics formalism described in Section 3. Thus,

we focus on the stress probability distribution function $P(\sigma,\zeta)$ which satisfies

$$\frac{\partial P}{\partial \zeta} = f(\zeta)\frac{\partial^2 P}{\partial \sigma^2}\,. \tag{14}$$

We assume that detachment occurs when the local stress on the length scale L/ζ reaches $-\sigma_{\rm a}(\zeta)$. Thus, the following boundary conditions are valid in the present case:

$$P(-\sigma_{\rm a}(\zeta),\zeta) = 0\,,$$

$$P(\infty,\zeta) = 0\,,$$

$$P(\sigma,1) = \delta(\sigma-\sigma_0)\,.$$

Let us write

$$s = \sigma + \sigma_{\rm a}(\zeta)\,.$$

If we denote $R(s,\zeta) = P(s-\sigma_{\rm a}(\zeta),\zeta)$, then (14) takes the form

$$\frac{\partial R}{\partial \zeta} + \frac{\partial R}{\partial s}\sigma_{\rm a}'(\zeta) = f(\zeta)\frac{\partial^2 R}{\partial s^2}\,, \tag{15}$$

where $R(s,\zeta)$ satisfies the boundary conditions

$$R(0,\zeta) = 0\,, \tag{16a}$$

$$R(\infty,\zeta) = 0\,, \tag{16b}$$

$$R(s,1) = \delta(s-\sigma_{\rm a}(1)-\sigma_0)\,. \tag{17}$$

Let us now solve equation (15). Let us first Laplace-transform the s-dependence:

$$\tilde R(z,\zeta) = \int_0^\infty {\rm d}s\ R(s,\zeta)e^{-sz}\,.$$

From (15), (16a) and (16b) we get

$$\frac{\partial \tilde R}{\partial \zeta} = \left[f(\zeta)z^2 - \sigma_{\rm a}'(\zeta)z\right]\tilde R - f(\zeta)g(\zeta)\,, \tag{18}$$

where $g(\zeta) = \partial R(s,\zeta)/\partial s|_{s=0}$. Let us introduce

$$a(\zeta) = \int_1^\zeta {\rm d}\zeta' f(\zeta')\,.$$

Equation (18) is easy to integrate:

$$\tilde R(z,\zeta) = A(z)\,\exp\left(a(\zeta)z^2 - \sigma_{\rm a}(\zeta)z\right)$$

$$-\int_1^\zeta {\rm d}\zeta'\ f(\zeta')g(\zeta')$$

$$\times\exp\left([a(\zeta)-a(\zeta')]z^2 - [\sigma_{\rm a}(\zeta)-\sigma_{\rm a}(\zeta')]z\right)\,. \tag{19}$$

The "initial condition" (17) gives

$$\tilde R(z,1) = \exp\left(-[\sigma_0+\sigma_{\rm a}(1)]z\right)\,.$$

Using this equation (19) gives

$$A(z) = e^{-\sigma_0 z}\,.$$

Substituting this result back in (19) gives

$$\tilde R(z,\zeta) = \exp\left(-[\sigma_0+\sigma_{\rm a}(\zeta)]z + a(\zeta)z^2\right)$$

$$-\int_1^\zeta {\rm d}\zeta'\ f(\zeta')g(\zeta')$$

$$\times\exp\left([a(\zeta)-a(\zeta')]z^2 - [\sigma_{\rm a}(\zeta)-\sigma_{\rm a}(\zeta')]z\right)\,.$$

Let us now return to s-space using

$$R(s,\zeta) = \frac{1}{2\pi i}\int_{-i\infty}^{i\infty}{\rm d}z\ \tilde R(z,\zeta){\rm e}^{sz}\,.$$

Using that

$$\frac{1}{2\pi i}\int_{-i\infty}^{i\infty}{\rm d}z\ e^{az^2-bz}\ e^{sz} = (4\pi a)^{-1/2}\exp\left(-\frac{(s-b)^2}{4a}\right)$$

gives

$$R(s,\zeta) = [4\pi a(\zeta)]^{-1/2}\exp\left(\frac{[s-\sigma_{\rm a}(\zeta)-\sigma_0]^2}{4a(\zeta)}\right)$$

$$-\int_1^\zeta {\rm d}\zeta'\ f(\zeta')g(\zeta')\,(4\pi[a(\zeta)-a(\zeta')])^{-1/2}$$

$$\times\ \exp\left(-\frac{(s-[\sigma_{\rm a}(\zeta)-\sigma_{\rm a}(\zeta')])^2}{4[a(\zeta)-a(\zeta')]}\right)\,.$$

The condition $R(0,\zeta)=0$ gives

$$\int_1^\zeta {\rm d}\zeta'\ f(\zeta')g(\zeta')\left(\frac{a(\zeta)}{a(\zeta)-a(\zeta')}\right)^{1/2}$$

$$\times\ \exp\left(-\frac{[\sigma_{\rm a}(\zeta)-\sigma_{\rm a}(\zeta')]^2}{4[a(\zeta)-a(\zeta')]}\right) =$$

$$\exp\left(-\frac{[\sigma_{\rm a}(\zeta)+\sigma_0]^2}{4a(\zeta)}\right)\,. \tag{20}$$

This is a linear integral equation for $g(\zeta)$ which is easy to solve by matrix inversion.

7 Distribution function P(ζ)

Let $P(\zeta)A_0$ be the area of real contact when the system is studied under the magnification ζ. The stress distribution is given by

$$P(\sigma,\zeta) = \langle\delta[\sigma-\sigma_1(\mathbf{x},\zeta)]\rangle$$

$$= \frac{1}{A_0}\int {\rm d}^2x\ \delta[\sigma-\sigma_1(\mathbf{x},\zeta)]\,,$$

where $\sigma_1(\mathbf{x},\zeta)$ is the stress in the contact area, for the surface roughness profile which is obtained by smoothening out roughness on length scales shorter than L/ζ, and where the integration is over the resulting area of real contact. Thus we get

$$\int_{-\sigma_{\rm a}}^\infty {\rm d}\sigma\ P(\sigma,\zeta) = \frac{A(\zeta)}{A_0}\,,$$

where $A(\zeta)$ is the area of real contact, projected in the xy-plane, which depends on the magnification ζ. Using the definition $P(\zeta) = A(\zeta)/A_0$ gives

$$P(\zeta) = \int_{-\sigma_a}^{\infty} \mathrm{d}\sigma\ P(\sigma,\zeta) = \int_0^{\infty} \mathrm{d}s\ R(s,\zeta)\,.$$

Integrating (14) over s and using $R(0,\zeta) = 0$ gives

$$\frac{\partial}{\partial\zeta}\int_0^{\infty} \mathrm{d}s\ R(s,\zeta) = \int_0^{\infty} \mathrm{d}s\ f(\zeta)\frac{\partial^2 R}{\partial s^2} = -f(\zeta)g(\zeta)\,.$$

Integrating this equation over ζ gives

$$\int_0^{\infty} \mathrm{d}s\ R(s,\zeta) = 1 - \int_1^{\zeta} \mathrm{d}\zeta'\ f(\zeta')g(\zeta')\,.$$

Thus

$$P(\zeta) = 1 - \int_1^{\zeta} \mathrm{d}\zeta'\ f(\zeta')g(\zeta')\,. \tag{21}$$

8 Analytical solution for $\sigma_a \equiv$ const

In order to make contact with the theory developed in reference [3] (see Sect. 3), let us assume that $\sigma_a(\zeta)$ is independent of ζ (in Ref. [3] we studied the case $\sigma_a \equiv 0$). In this case (20) takes the form

$$\int_1^{\zeta} \mathrm{d}\zeta'\ f(\zeta')g(\zeta')\left(\frac{a(\zeta)}{a(\zeta)-a(\zeta')}\right)^{1/2} = \exp\left(-\frac{[\sigma_a+\sigma_0]^2}{4a(\zeta)}\right)\,. \tag{22}$$

If we introduce as a new integration variable,

$$a(\zeta) = \int_1^{\zeta} \mathrm{d}\zeta'\ f(\zeta'), \qquad \mathrm{d}a = f(\zeta)\mathrm{d}\zeta\,,$$

and consider $g(\zeta)$ as a function of a (denoted by $g(a)$ for simplicity) then (22) takes the form

$$\int_0^{a} \mathrm{d}a'\ g(a')\left(\frac{a}{a-a'}\right)^{1/2} = \exp\left(-\frac{[\sigma_a+\sigma_0]^2}{4a}\right)\,. \tag{23}$$

This integral equation has the solution

$$g(a) = (4\pi a)^{-1/2}\,\frac{\sigma_0+\sigma_a}{a}\exp\left(-\frac{[\sigma_0+\sigma_a]^2}{4a}\right)\,. \tag{24}$$

It is easy to prove that (24) is a solution to (23) by substituting (24) in (23) and change integration variable from a' to x where

$$x^2 = \frac{1}{a'} - \frac{1}{a}.$$

Substituting (24) in (21), changing integration variable first from ζ' to $a' = a(\zeta')$, and then writing $x^2 = (\sigma_0 + \sigma_a)^2/a'$ gives

$$P(\zeta) = \frac{1}{\sqrt{\pi}}\int_0^{1/\sqrt{G}} \mathrm{d}x\ e^{-x^2/4} = \mathrm{erf}\,(1/2\sqrt{G})\ , \tag{25}$$

where $G(\zeta) = a(\zeta)/(\sigma_0+\sigma_a)^2$. It is easy to show that (25) also can be written in the form

$$P(\zeta) = \frac{2}{\pi}\int_0^{\infty} \mathrm{d}x\ \frac{\sin x}{x}e^{-x^2G}\,. \tag{26}$$

In order to prove that (25) and (26) are identical, let us denote $q = 1/\sqrt{G}$ and replace $x = qy$ in (26). If we consider the integral as a function of q and write

$$I(q) = \frac{2}{\pi}\int_0^{\infty} \mathrm{d}y\ \frac{\sin(qy)}{y}e^{-y^2}\,,$$

then

$$I'(q) = \frac{2}{\pi}\int_0^{\infty} \mathrm{d}y\ \sin(qy)\ e^{-y^2} = \frac{1}{\sqrt{\pi}}e^{-q^2/4}\,,$$

Integrating this equation gives

$$I(q) = \frac{1}{\sqrt{\pi}}\int_0^{q} dx\ e^{-x^2/4}\,,$$

which agrees with (25) if we replace $q = 1/\sqrt{G}$. Equation (26) (with $\sigma_a = 0$) was derived in reference [3] using a different method and we have shown that the present formalism gives the same result when σ_a is a constant. We note that for small effective load $\sigma_0 + \sigma_a$ we have $G \gg 1$ for large enough ζ, and in this case only $x \ll 1$ will contribute in the integral (26) and we can replace $\sin x \approx x$ to get

$$P(\zeta) \approx [\pi G(\zeta)]^{-1/2} \sim \sigma_0 + \sigma_a\,.$$

Thus, in this limit the area of real contact is proportional to the sum of the applied pressure σ_0 and the "adhesion" pressure σ_a. This result has often been used [19], *e.g.*, in discussing friction, but we point out that it is only valid when $\sigma_a(\zeta)$ is independent of ζ. This will never be the case when surface roughness occurs on many different length scales (see below).

9 Detachment stress $\sigma_a(\zeta)$

Let us consider the system on the characteristic length scale $\lambda = L/\zeta$. The quantity $\sigma_a(\zeta)$ is the stress necessary to induce a detached area of width λ. This stress can be obtained from the following standard arguments related to a penny-shaped crack of diameter λ. To create an interfacial crack of width λ requires the surface energy $\sim\ \gamma_{\rm eff}(\zeta)\lambda^2$. On the other hand, the crack formation lowers the elastic energy in a volume element of order λ^3 from the value (per unit volume) $\sim \sigma_a^2/E$ before detachment to ≈ 0 after detachment. The detachment stress σ_a is determined by the fact that the free energy change

$$U \approx \gamma_{\rm eff}\lambda^2 - \sigma_a^2\lambda^3/E$$

is an extremum, which gives

$$\sigma_a \approx \left[\frac{2\gamma_{\rm eff}(\zeta)E}{3\lambda}\right]^{1/2}\,.$$

An exact calculation gives [20]

$$\sigma_{\rm a} = \left[\frac{\pi\gamma_{\rm eff}(\zeta)E}{(1-\nu^2)\lambda}\right]^{1/2} = \left[\frac{\gamma_{\rm eff}(\zeta)Eq}{2(1-\nu^2)}\right]^{1/2}, \qquad (27)$$

where $q = 2\pi/\lambda = \zeta q_L$.

Note that when we consider the system on the length scale λ, surface roughness of length scales shorter than λ is contained in $\gamma_{\rm eff}(\lambda)$ and should therefore not be included in the discussion. Thus, the surfaces are effectively smooth on length scales shorter than λ. When we consider the system on the length scale λ detached areas will have a diameter of order λ or larger (detached areas with smaller diameter may also occur, but this has already been taken into account in the effective surface energy $\gamma_{\rm eff}(\lambda)$). The detached areas with diameter larger than λ, say λ_1, are taken into account separately when the argument above is applied to the length scale λ_1.

10 Effective surface energy $\gamma_{\rm eff}(\zeta)$

We now derive an expression for $\gamma_{\rm eff}(\zeta)$ which is the effective surface energy change upon contact. Suppose first that the elastic body makes perfect contact with the hard rough substrate. In that case we can use the result of Section 4 with q_0 replaced with $q_{\rm a}$ so that the effective surface energy on the length scale $\lambda_{\rm a} = L/\zeta_{\rm a}$ is given by

$$\gamma_{\rm eff}(q_{\rm a}) = \Delta\gamma\left[\int_0^\infty {\rm d}x\ \left(1+\xi^2 x\right)^{1/2} e^{-x} - \frac{2\pi}{\delta}\int_{q_{\rm a}}^{q_1} {\rm d}q\ q^2 C(q)\right]. \qquad (28)$$

In (28), q_1 is the short-distance cut-off wave vector which is of order of (or smaller than) $2\pi/a$, where a is a lattice constant. Let us now take into account that only partial contact occurs on each length scale. Thus we get

$$\gamma_{\rm eff}(q_{\rm a})P(q_{\rm a}) = \Delta\gamma\left[P(q_1)\int_0^\infty {\rm d}x\ \left(1+\xi^2 x\right)^{1/2} e^{-x} - \frac{2\pi}{\delta}\int_{q_{\rm a}}^{q_1} {\rm d}q\ q^2 P(q)C(q)\right]$$

or

$$\frac{\gamma_{\rm eff}(q_a)}{\Delta\gamma} = \frac{P(q_1)}{P(q_{\rm a})}\int_0^\infty {\rm d}x\ \left(1+\xi^2 x\right)^{1/2} e^{-x} - \frac{2\pi}{\delta}\int_{q_{\rm a}}^{q_1} {\rm d}q\ q^2\frac{P(q)}{P(q_{\rm a})}C(q). \qquad (29)$$

11 Adhesion for self-affine fractal surfaces

The theory developed above assumes surface roughness on many length scales characterized by the power spectra $C(q)$. In practical applications, the measured $C(q)$ can be used directly as input in the calculations. In what follows we will assume that the surfaces are self-affine fractal. In this section we give the basic equations for this limiting case. Let us first summarize the equations derived above: The relative contact area (at the magnification ζ) is given by

$$P(\zeta) = 1 - \int_1^\zeta {\rm d}\zeta'\ S(\zeta'), \qquad (30)$$

where $S(\zeta) = f(\zeta)g(\zeta)$, where $S(\zeta)$ is obtained from the integral equation

$$\int_1^\zeta {\rm d}\zeta'\ S(\zeta')\left(\frac{a(\zeta)}{a(\zeta)-a(\zeta')}\right)^{1/2} \times \exp\left(-\frac{[\sigma_{\rm a}(\zeta)-\sigma_{\rm a}(\zeta')]^2}{4[a(\zeta)-a(\zeta')]}\right) = \exp\left(-\frac{[\sigma_{\rm a}(\zeta)+\sigma_0]^2}{4a(\zeta)}\right), \qquad (31)$$

where

$$a(\zeta) = \int_1^\zeta {\rm d}\zeta'\ f(\zeta'), \qquad (32)$$

$$f(\zeta) = \frac{\pi}{4}q_L q^3 C(q)\left(\frac{E}{1-\nu^2}\right)^2. \qquad (33)$$

Equation (31) is a linear integral equation for $S(\zeta)$ which is easy to solve by matrix inversion. The detachment stress $\sigma_{\rm a}(\zeta)$ on the length scale L/ζ is given by

$$\sigma_{\rm a} \approx \left[\frac{\gamma_{\rm eff}(\zeta)Eq}{2(1-\nu^2)}\right]^{1/2}. \qquad (34)$$

The effective surface energy $\gamma_{\rm eff}(\zeta)$ is given by equation (29):

$$\frac{\gamma_{\rm eff}(q_{\rm a})}{\Delta\gamma} = \frac{P(q_1)}{P(q_{\rm a})}\int_0^\infty {\rm d}x\ \left(1+\xi^2 x\right)^{1/2} e^{-x} - \frac{2\pi}{\delta}\int_{q_{\rm a}}^{q_1} {\rm d}q\ q^2\frac{P(q)}{P(q_{\rm a})}C(q). \qquad (35)$$

The system of equations above are easy to solve by iteration.

We assume in what follows that $C(q)$ corresponds to a self-affine fractal surface. Substituting (10) in (32) and denoting $q = q_0\zeta$ we get

$$a(\zeta) = \frac{(q_0 h_0)^2 H}{16(1-H)}\left(\frac{E}{1-\nu^2}\right)^2\left(\zeta^{2(1-H)}-1\right). \qquad (36)$$

Let us define

$$\bar{a}(\zeta) = \zeta^{2(1-H)} - 1$$

and

$$\bar{\sigma}_{\rm a} = \sigma_{\rm a}\frac{4}{q_0 h_0}\left(\frac{1-H}{H}\right)^{1/2}\frac{1-\nu^2}{E}$$

and similar for $\bar{\sigma}_0$. Thus, (31) takes the form

$$\int_1^\zeta \mathrm{d}\zeta'\ S(\zeta')\left(\frac{\bar{a}(\zeta)}{\bar{a}(\zeta)-\bar{a}(\zeta')}\right)^{1/2} \times\exp\left(-\frac{[\bar{\sigma}_{\rm a}(\zeta)-\bar{\sigma}_{\rm a}(\zeta')]^2}{4[\bar{a}(\zeta)-\bar{a}(\zeta')]}\right)= \exp\left(-\frac{[\bar{\sigma}_{\rm a}(\zeta)+\bar{\sigma}_0]^2}{4\bar{a}(\zeta)}\right). \quad (37)$$

Using (34) we get

$$\bar{\sigma}_{\rm a}^2=\frac{2(1-H)}{H}\frac{\zeta q_0\delta}{(q_0h_0)^2}\frac{\gamma_{\rm eff}(\zeta)}{\Delta\gamma}. \quad (38)$$

The effective interfacial energy takes the form

$$\frac{\gamma_{\rm eff}(\zeta_{\rm a})}{\Delta\gamma}=\frac{P(\zeta_1)}{P(\zeta_{\rm a})}\int_0^\infty \mathrm{d}x\ \left(1+\xi^2x\right)^{1/2}e^{-x} -H\frac{(q_0h_0)^2}{q_0\delta}\int_{\zeta_{\rm a}}^{\zeta_1}\mathrm{d}\zeta\ \zeta^{-2H}\frac{P(\zeta)}{P(\zeta_{\rm a})}, \quad (39)$$

where

$$\xi^2=(q_0h_0)^2\frac{H}{2(1-H)}\left(\zeta_1^{2(1-H)}-\zeta_{\rm a}^{2(1-H)}\right).$$

Note that

$$\int_0^\infty \mathrm{d}x\left(1+\xi^2x\right)^{1/2}\mathrm{e}^{-x}=1+\frac{\sqrt{\pi}}{2}\xi\left[1-\mathrm{erf}\left(\xi^{-1}\right)\right]\exp\left(\xi^{-2}\right).$$

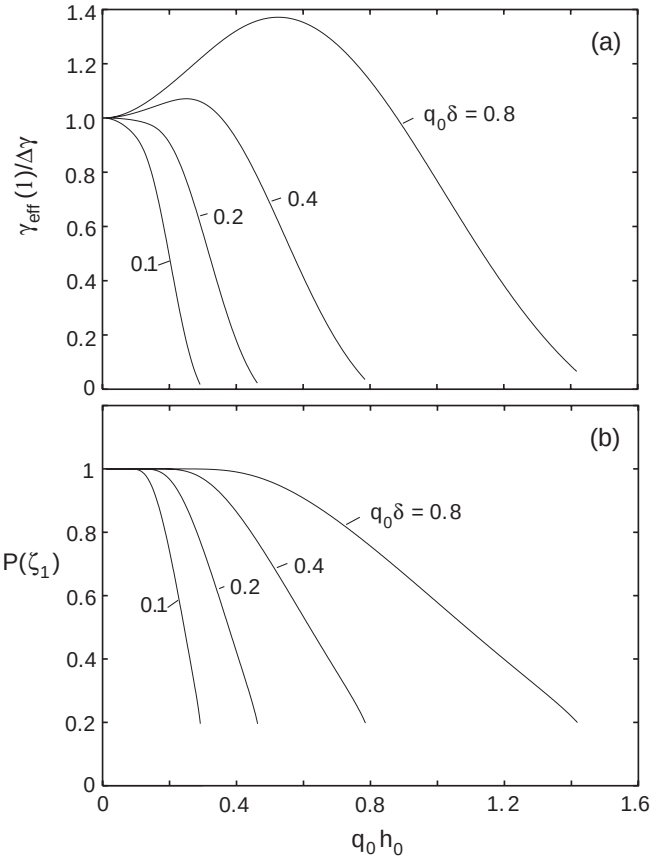

Fig. 9. (a) The macroscopic interfacial energy as a function of q_0h_0. (b) The normalized area of real contact, $P(\zeta_1)=A(\zeta_1)/A_0$, as a function of of q_0h_0. For $q_0\delta=0.1$, 0.2, 0.4 and 0.8 as indicated. For $H=0.8$ and $q_1/q_0=\zeta_1=100$.

12 Numerical results

Let us now present numerical results obtained from (30), (37-39) by iteration. We assume that the rough surface is self-affine fractal with the Hurst exponent H corresponding to the fractal dimension $D_{\rm f}=3-H$. We consider first the case $H=0.8$ or $D_{\rm f}=2.2$, as is typical for many surfaces of practical interest, *e.g.*, surfaces prepared by fracture or sand-blasting, and we first assume $\zeta_1=q_1/q_0=100$. In what follows we assume, unless otherwise stated, that the external load vanishes.

Figure 9 shows (a) the effective interfacial energy $\gamma_{\rm eff}(1)$ and (b) the normalized area of real contact, $P(\zeta_1)=A(\zeta_1)/A_0$, as a function of of q_0h_0. Results are shown for $q_0\delta=0.1$, 0.2, 0.4 and 0.8. We will refer to $\gamma_{\rm eff}(1)$ at the magnification $\zeta=1$ as the *macroscopic* interfacial free energy which can be deduced from, *e.g.*, the pull-off force for a ball according to equation (13). Note that for $q_0\delta=0.4$ and 0.8 the macroscopic interfacial energy first increases with increasing amplitude h_0 of the surface roughness, and then decreases. The increase in $\gamma_{\rm eff}$ arises from the increase in the surface area. Since the solid-solid contact is complete for small h_0 (see Fig. 9(b)) we can use the criteria derived in Section 4 that the adhesion force increases with increasing h_0 (for small h_0) when $q_0\delta>\alpha(H)$: in the present case $\alpha(0.8)=0.235$ (see Sect. 4) so that the adhesion force should initially increase with increasing h_0 for $q_0\delta=0.4$ and 0.8, but not for $q_0\delta=0.1$ and 0.2, in agreement with Figure 9(a). As shown in Figure 9(b), for small h_0 the two solids are in complete contact, and, as expected, the complete contact remains to higher h_0 as $\delta\sim\Delta\gamma/E$ increases. Note also that the contact area is non-zero even when $\gamma_{\rm eff}(1)$ is virtually zero: the fact that $\gamma_{\rm eff}(1)$ (nearly) vanishes does not imply that the contact area vanishes (even in the absence of an external load), but implies that the (positive) elastic energy stored at the interface just balances the (negative) adhesion energy from the area of real contact. The stored elastic energy at the interface is given back when removing the block, and when $\gamma_{\rm eff}(1)\approx0$ it is just large enough to break the block-substrate bonding.

Figure 10 shows (a) the effective interfacial energy $\gamma_{\rm eff}(\zeta)$, and (b) the normalized area of (apparent) contact, $P(\zeta)=A(\zeta)/A_0$, as a function of the magnification ζ. Note that at short length scale (large ζ) $\gamma_{\rm eff}(\zeta)$ increases with decreasing magnification. This effect results from the increase in the contact area as more and more of the short-wavelength roughness components are taken into account (or "integrated out"). However, at long enough length scale, close to the long-distance cut-off length λ_0

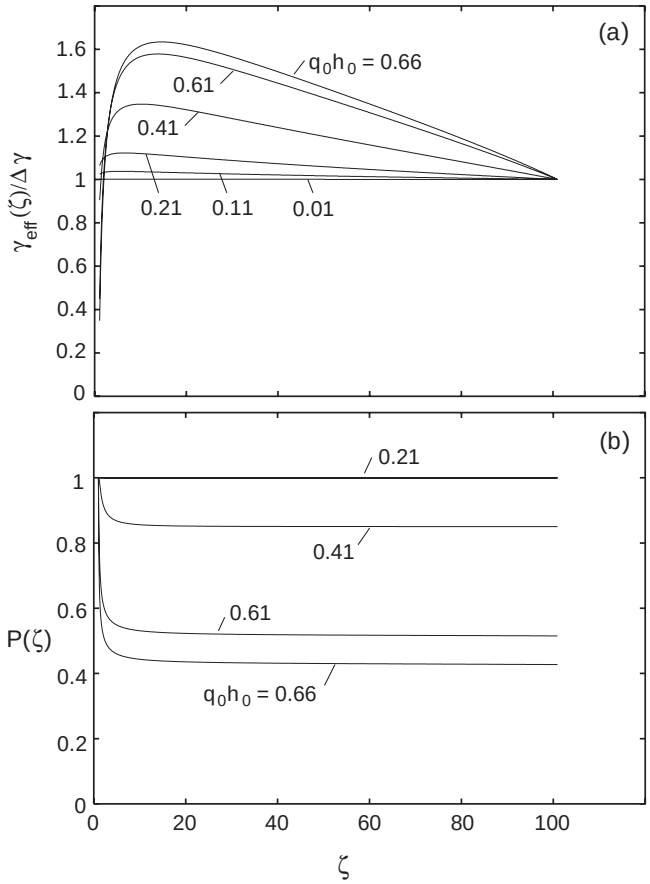

Fig. 10. (a) The effective interfacial energy as a function of the magnification ζ. (b) The normalized (apparent) area of contact, $P(\zeta) = A(\zeta)/A_0$, as a function of the magnification ζ. The curves correspond to different values of q_0h_0 as indicated. For $q_0\delta = 0.4$, $H = 0.8$ and $\zeta_1 = 100$.

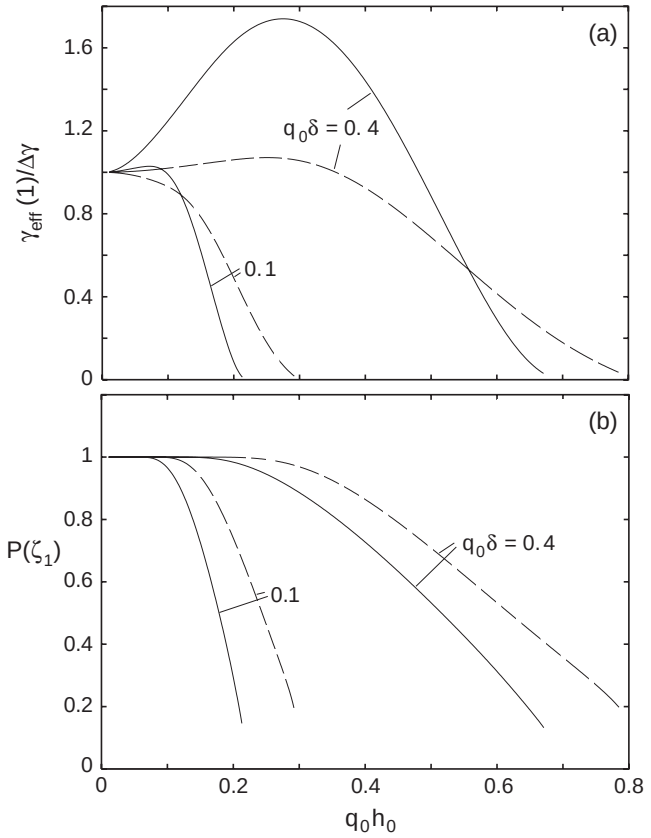

Fig. 11. (a) The macroscopic adhesion energy as a function of q_0h_0. (b) The normalized area of real contact, $P(\zeta_1) = A(\zeta_1)/A_0$, as a function of of q_0h_0. The solid and dashed curves correspond to $H = 0.4$ and 0.8, respectively. For $q_0\delta = 0.1$ and 0.4 as indicated, and $q_1/q_0 = \zeta_1 = 100$.

(which corresponds to the magnification $\zeta = 1$), $\gamma_{\rm eff}(\zeta)$ becomes smaller than $\Delta\gamma$. This effect results from the contribution to the interfacial free energy from the roughness-induced elastic deformation energy stored in the rubber at the interface (see Sect. 4). Since the elastic energy per unit contact area scales as $\sim \lambda^{5-2D_{\rm f}}$, for $D_{\rm f} < 2.5$ the longest-wavelength surface roughness components will give a larger contribution to the stored elastic energy than the short-wavelength components, and this is the reason why $\gamma_{\rm eff}$ decreases close to the long-distance cut-off λ_0. Note also that $\gamma_{\rm eff}(\zeta)$ at the shortest length scale (which in the present case corresponds to the magnification $\zeta = 100$) equals the "bare" value $\Delta\gamma$ as it should.

Figure 10(b) shows that, with increasing magnification, the (normalized) area of (apparent) contact, $P(\zeta)$, reaches a constant value already for $\zeta \approx 10$. This implies that when a contact area at the magnification ~ 10 is studied at higher magnification (where smaller-scale roughness structures or bumps are seen), the rubber will be in perfect contact with the substrate (see Fig. 13(a) below). This is no longer the case when the fractal dimension of the surface is higher. Thus we will show below that for $D_{\rm f} = 2.4$ (instead of $D_{\rm f} = 2.2$ used in Fig. 10), $P(\zeta)$ decreases continuously with increasing magnification (see Fig. 13(b) below).

Figure 11 shows (a) the macroscopic interfacial energy $\gamma_{\rm eff}(1)$ and (b) the normalized area of real contact, $P(\zeta_1) = A(\zeta_1)/A_0$, as a function of q_0h_0. We show results for both $H = 0.4$ (solid lines) and 0.8 (dashed lines), for $q_0\delta = 0.1$ and 0.4. Note that the enhancement in the adhesion for small h_0 is much larger for $H = 0.4$ than for 0.8; this result is expected since (see Sect. 4) $\alpha(0.4) = 0.073$ and $\alpha(0.8) = 0.235$ so that $\alpha(0.4) \ll \alpha(0.8)$. Physically, it comes about because the roughness-induced increase in the surface area is much larger when $H = 0.4$ than for $H = 0.8$ and this will enhance the adhesive contribution to the macroscopic interfacial energy $\gamma_{\rm eff}$ (see below). For $H = 0.4$ we observe an increase in $\gamma_{\rm eff}$ for small h_0 for both $q_0\delta = 0.1$ and 0.4 which is consistent with the value $\alpha(0.4) = 0.073$ given above.

Figure 12 shows (a) the effective interfacial energy $\gamma_{\rm eff}(\zeta)$ and (b) the normalized area of real contact, $P(\zeta) = A(\zeta)/A_0$, as a function of the magnification ζ. The curves correspond to different values of q_0h_0 as indicated, and with $q_0\delta = 0.4$ and $H = 0.4$. Compared to Figure 10, note the much more rapid increase in $\gamma_{\rm eff}(\zeta)$ when the magnification ζ is reduced from the short-distance cut-off $\zeta_1 = 100$. Figure 12(b) shows that in the present case

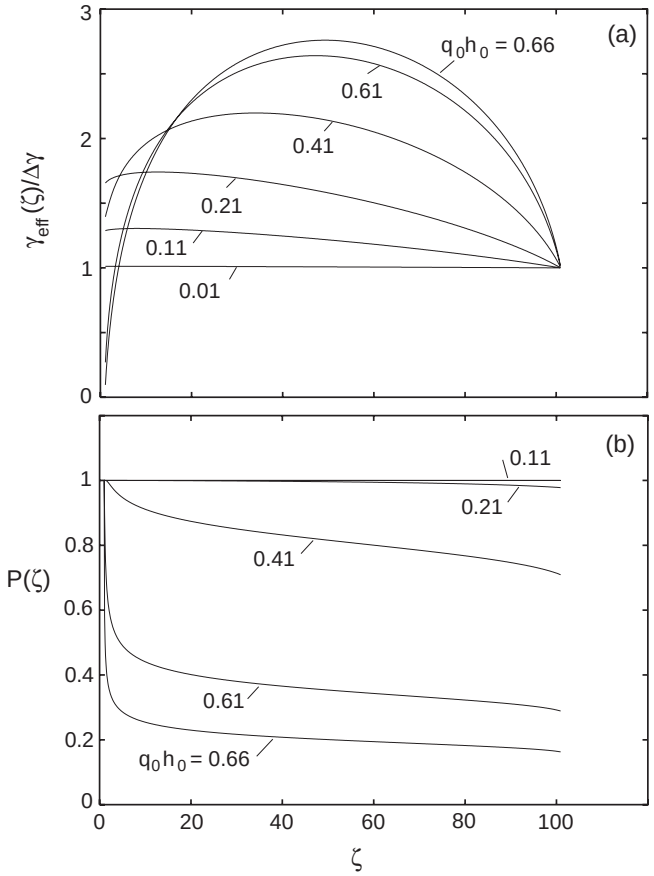

Fig. 12. (a) The effective interfacial energy as a function of the magnification ζ. (b) The normalized area of real contact, $P(\zeta) = A(\zeta)/A_0$, as a function of the magnification ζ. The curves correspond to different values of q_0h_0 as indicated. For $q_0\delta = 0.4$ and $H = 0.4$.

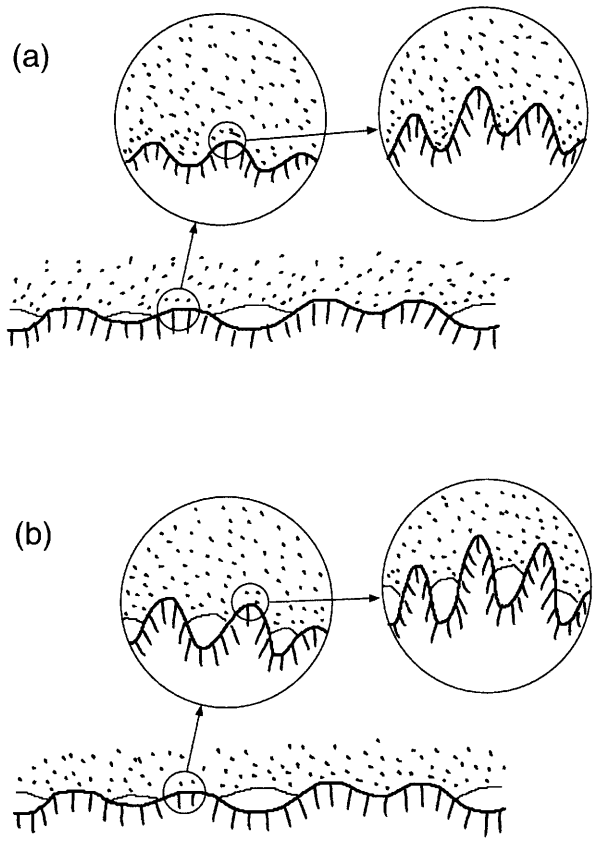

Fig. 13. The adhesive contact between an elastic body (dotted area) and a hard rough substrate (dashed area). (a) When the roughness exponent H is larger than 1/2 (corresponding to a fractal dimension $2 < D_f < 2.5$) complete contact occurs in the macro-asperity contact areas. (b) When the roughness exponent H is smaller than 1/2 (corresponding to a fractal dimension $2.5 < D_f < 3$), at all magnifications only partial contact occurs in the macro-asperity contact areas. (Schematic.)

where the fractal dimension $D_f = 2.6$, the area of (apparent) contact decreases *continuously* with increasing magnification. This is in sharp contrast to the case where $D_f = 2.2$, where $P(\zeta)$ is constant for $\zeta > 10$. The origin of this difference is explained qualitatively in Figure 13.

Figure 13 shows (schematically) the adhesive contact between an elastic body (dotted area) and a hard rough substrate (dashed area). In (a) the roughness exponent H is close to 1 (the fractal dimension D_f close to 2) in which case complete contact occurs in the macro-asperity contact areas. In (b) the roughness exponent H is smaller than 1/2 (corresponding to a fractal dimension $D_f > 2.5$), and at all magnifications only partial contact occurs in the macro-asperity contact areas. The difference between the two cases was described qualitatively in Section 2. Here we give an additional argument. We will show that for large fractal dimension the amplitude h of the roughness, at the (fixed) length scale λ, is much larger than when the fractal dimension is close to 3, as illustrated in Figure 13. This is easy to prove as follows. For two surfaces with equal h_0 and λ_0 (*i.e.*, equal rms roughness and equal long-distance cut-off length) but different Hurst exponents H and H' we get for the roughness amplitudes h and h' on the length scale λ:

$$h_0/\lambda_0 = (h/\lambda)(\lambda/\lambda_0)^{1-H} = (h'/\lambda)(\lambda/\lambda_0)^{1-H'}$$

or

$$h/h' = (\lambda/\lambda_0)^{D'_f - D_f}\,.$$

Thus, if $D'_f > D_f$ we get $h' > h$. The large value of h/λ at high resolution when D_f is "large" (say larger than 2.5) will in general result in a monotonic decrease in the (apparent) contact area as the magnification is increased. Without a short distance cut-off, the area of real contact and hence the adhesion interaction will likely vanish. (This is only true as long as the adhesion interaction between the two solids is assumed to have an infinitesimal extent so that interaction only occurs when the solids are in *direct* contact. This is a good approximation for covalent or metallic interactions, but not for the more long-ranged van der Waals interaction, see Ref. [2].)

Figure 14 (a) shows the macroscopic interfacial energy and (b) the normalized area of real contact, $P(\zeta_1) = A(\zeta_1)/A_0$, as a function of of q_0h_0. The curves denoted by a and b correspond to the external pressure

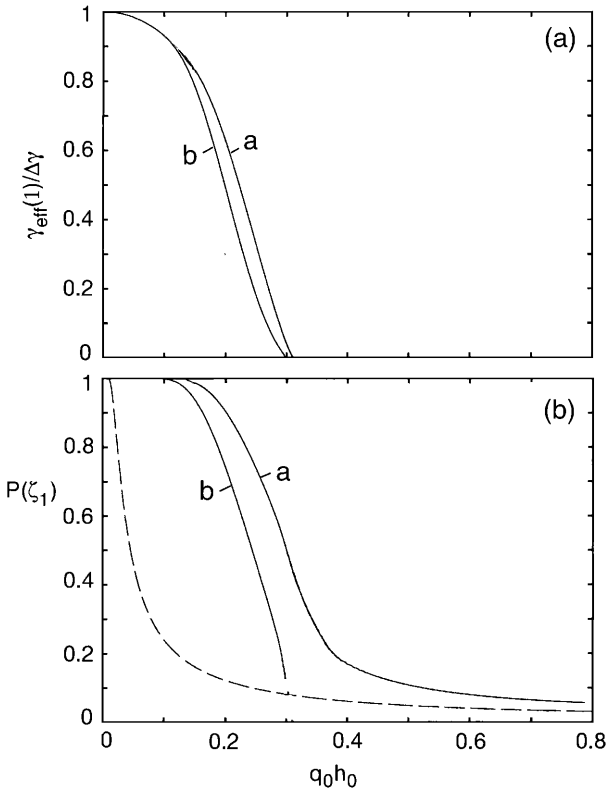

Fig. 14. (a) The macroscopic interfacial energy as a function of q_0h_0. (b) The normalized area of real contact, $P(\zeta_1) = A(\zeta_1)/A_0$, as a function of of q_0h_0. The curves denoted by a and b correspond to the external pressure $\sigma_0 = 0.05E/(1-\nu^2)$ and $\sigma_0 = 0$, respectively. In (b) the dashed line is for no adhesion (*i.e.*, $\Delta\gamma = 0$), and for the same external pressure as for curve a. For $H = 0.8$, $q_0\delta = 0.1$ and $q_1/q_0 = \zeta_1 = 100$.

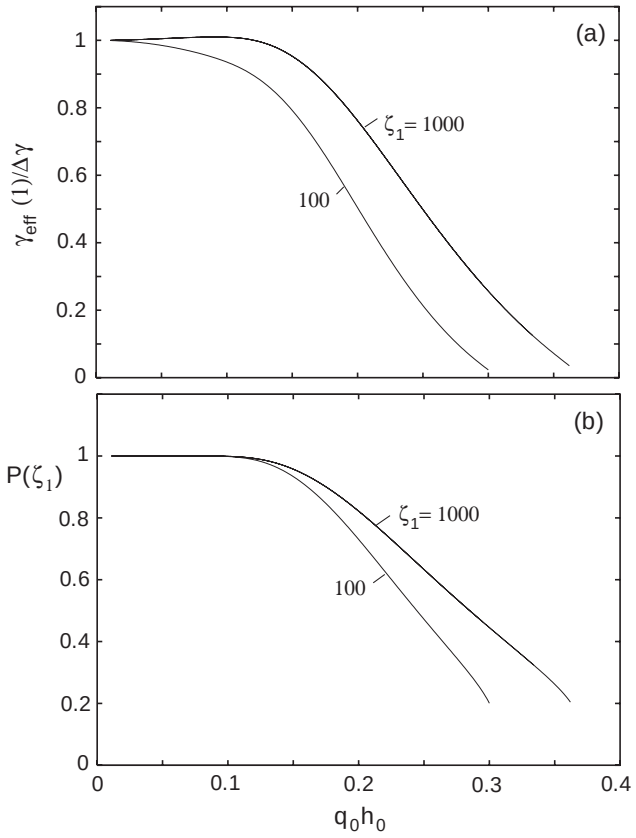

Fig. 15. (a) The macroscopic interfacial energy as a function of q_0h_0. (b) The normalized area of real contact, $P(\zeta_1) = A(\zeta_1)/A_0$, as a function of of q_0h_0. Results are shown for $q_1/q_0 = \zeta_1 = 100$ and 1000. For $H = 0.8$ and $q_0\delta = 0.1$.

$\sigma = 0.05E/(1-\nu^2)$ and $\sigma = 0$, respectively. In (b) the dashed line is for no adhesion (*i.e.*, $\Delta\gamma = 0$), and for the same external pressure as for curve a. Note that with increasing h_0, the area of real contact (when adhesion is included) only very slowly approaches the contact area which would result when the adhesion is neglected (dashed line). Since it is the area of real contact which is important in sliding friction, it is clear that the adhesion interaction may strongly affect the friction force even when no adhesion can be detected in a pull-off experiment; in the present case, $\gamma_{\rm eff}(1)$ and hence the pull-off force vanish when $q_0h_0 = 0.3$ but even when $q_0h_0 = 0.5$, the area of real contact is more than twice as large when the adhesion is included as when it is neglected.

The variation of $P(\zeta)$ and $\gamma_{\rm eff}(\zeta)$ with the magnification ζ, for the same system as in Figure 14, is shown in Figures 3 and 5. In Figure 3 we show $P(\zeta)$ both with and without adhesion and for the squeezing pressure $\sigma_0 = 0.05E/(1-\nu^2)$. Note that without the adhesion, $P(\zeta)$ decreases monotonically with increasing magnification, and, in fact, without a short-distance cut-off, the area of real contact (corresponding to $P(\infty)$) vanishes. When adhesion is included, the (apparent) area of contact equals the area of real contact already at a rather small magnification $\zeta \approx 10$. The result for $\gamma_{\rm eff}$ is similar to the results presented in Figure 10.

Figure 15 shows (a) the macroscopic adhesion energy and (b) the normalized area of real contact, $P(\zeta_1) = A(\zeta_1)/A_0$, as a function of of q_0h_0. Results are shown for $q_1/q_0 = \zeta_1 = 100$ and 1000. Note that for $\zeta_1 = 1000$, $\gamma_{\rm eff}(1)$ initially increases with increasing q_0h_0. This is the expected result since $\alpha(0.8) = 0.088$ for $\zeta_1 = 1000$ (see Sect. 4) so that $\alpha(0.8) < q_0\delta$ and the observed result follows from the theory in Section 4.

13 Comparison with experiment and discussion

The theory of adhesion presented above requires as input the 2D surface roughness power spectra $C(q)$. This quantity can now be routinely measured using, *e.g.*, the atomic-force microscopy. We note that when the surface roughness is isotropic, $C(q)$ can be obtained directly from the 1D power spectra. Suppose that the height $h(x)$ has been measured along a line (x-axis). We define the 1D height-height correlation function by

$$C_{\rm 1D}(x) = \langle h(x)h(0)\rangle\,,$$

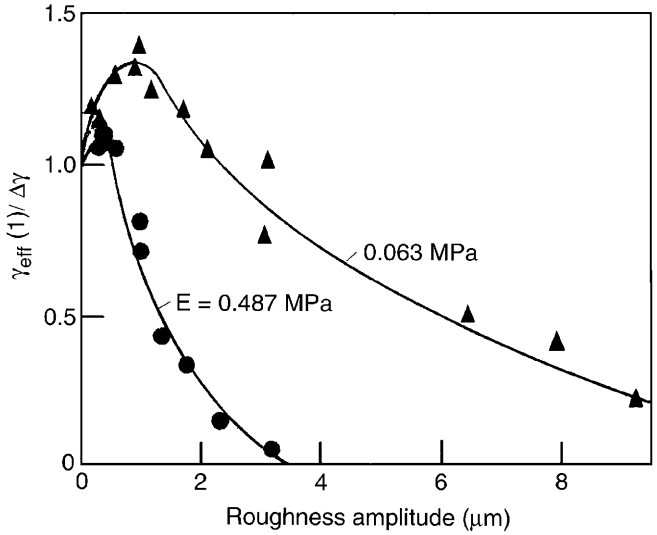

Fig. 16. The macroscopic interfacial energy (obtained from the pull-off force) for a smooth rubber surface (ball) in contact with Perspex surface as a function of the roughness (center line average) of the Perspex. Results are shown for a "soft" rubber ($E = 0.063$ MPa) and a "hard" rubber ($E = 0.487$ MPa). From [5].

where we have assumed that $\langle h(x)\rangle = 0$. If the surface roughness is isotropic, then $\langle h(\mathbf{x})h(\mathbf{0})\rangle = C_{1\mathrm{D}}(r)$, where $r = |\mathbf{x}|$. Thus we get

$$C(q) = \frac{1}{(2\pi)^2}\int \mathrm{d}^2x\ \langle h(\mathbf{x})h(\mathbf{0})\rangle e^{-i\mathbf{q}\cdot\mathbf{x}}$$

$$= \frac{1}{2\pi}\int_0^\infty \mathrm{d}r\ rC_{1\mathrm{D}}(r)J_0(qr)\,,$$

where $J_0(x)$ is the zeroth-order Bessel function.

Unfortunately, the surface roughness power spectra have not been measured for any surface for which adhesion has been studied in detail. Instead, only the roughness amplitude (center line average) and the radius of curvature of the largest surface asperities were determined. Nevertheless, the experimental data of Fuller, Tabor, Briggs, Briscoe and Roberts are in good qualitative agreement with our theoretical results. In Figure 16 we show the macroscopic interfacial energy for "hard" and "soft" rubber in contact with Perspex, as a function of the substrate (Perspex) roughness amplitude as obtained by Briggs and Briscoe [5]. It is not possible to compare these results quantitatively with the theory developed above since the power spectra $C(q)$ were not measured for the Perspex substrate. Even if the surfaces would be self-affine fractal as assumed in Section 12, not only the surface roughness amplitude will change from one surface to another, but so will the long-distance cut-off length λ_0 and hence also the ratio $\zeta_1 = q_1/q_0$. In the experiments reported on in reference [5] the Perspex surfaces were roughened by blasting with fine particles. The roughness could be varied by choice of the particles and the air pressure.

I suggest that a detailed study of adhesion is performed on surfaces for which $C(q)$ has been measured. One way of generating rough surfaces is to start with a smooth surface and sputter or sand blasting the surface. This will generate surfaces which most likely are (approximately) self-affine with a rms roughness amplitude and cut-off length λ_0 which change with the sputter or sand blasting conditions. Alternatively, self-affine fractal surfaces can be prepared by depositing atoms on an initially smooth substrate, see *e.g.*, reference [22].

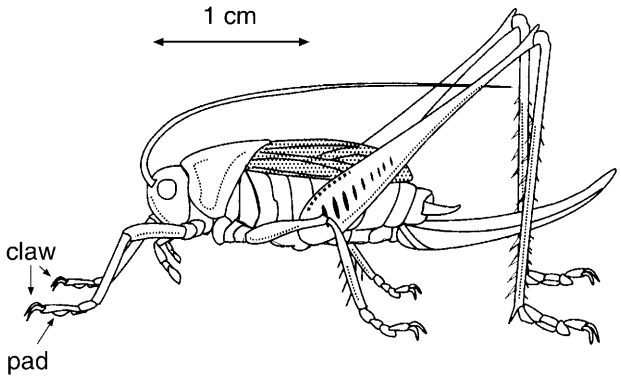

Fig. 17. The great green bush cricket. The attachment pads were the subject of the study focusing on indentation, adhesion and friction, reported on in reference [21].

One practical problem is that most rubber materials have a wide distribution of relaxation times, extending to extremely long times. This effect is well known in the context of rubber friction, where measurements of the complex elastic modulus show an extremely wide distribution of relaxation times, resulting in large sliding friction even at very low sliding velocities, $v < 10^{-8}$ m/s. The same effect has been observed in other experiments, see, *e.g.*, references [23,24].

We have seen in Section 12 that already a relative small roughness can completely remove (or "kill") the adhesion between two elastic bodies. One way of "restoring" a strong adhesion is to introduce a very thin layer of a wetting liquid at the interface, which is able to fill out the surface roughness "cavities" resulting in a strong liquid-mediated adhesion between the solid walls. This fact is made use of in many biological systems.

Some living objects, *e.g.*, tree frogs, some bats, crickets and many flies, have attachment pads on their legs which are responsible for attachment to the substrate during climbing on smooth substrates, *e.g.*, a fly climbing on a window glass or a cricket on a smooth leaf of a plant.

Recently, a detailed study has been performed on the attachment pads of the great green bush cricket [21], see Figure 17. The attachment system is designed to hold the insect on a rough surface, *e.g.*, the bark on a tree, using small claws at the end of each leg (see Fig. 17). To adhere to a smooth surface, *e.g.*, the leaves of many plant species, the insect uses attachment pads. The pads are nearly hemispherical with a radius of order ~ 2 mm and are elastically very soft with an effective elastic modulus determined from indentation experiments to be of order 0.02 MPa, *i.e.*, similar to very soft rubber. (Thus, $E \ll E_\mathrm{c}$, and the pads are "sticky".) The

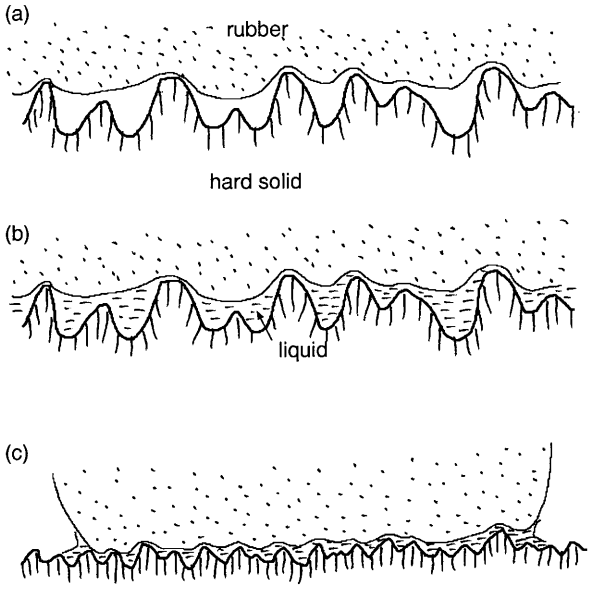

Fig. 18. (a) For very rough surfaces, the area of real contact is very small, and the adhesion is negligible. (b) In this case a thin fluid film may enhance the effective adhesion by bridging the gap between the surfaces. During "rapid" pull-off, a large negative pressure may occur in the fluid because there is not enough time for it to flow into the space between the surfaces during separation; this effect is particularly important when the fluid has a large viscosity, and when the fluid film is very thin. (c) The fluid film forms a capillary bridge between the solids giving a strong effective adhesion which is independent of the separation speed. The insect pad-substrate adhesion will in general depend on both effects (b) and (c). Similar effects may occur when a rubber block is in contact with a substrate, where the liquid now may be derived from contamination, or from out-diffusion (sweating) of liquid components from the rubber matrix.

pads deform purely elastically (no plastic or permanent deformation) even during deformations involving strains of order $\sim 100\%$ or more, and when the applied force is removed the deformed pads relax back to their original (undeformed) state.

The attachment system of the cricket is supported by a secretion produced by cells in the outer layer of the skin and transported onto the pad surface through pore canals. The secretion liquid is an organic liquid with hydrophilic properties. However, the liquid does wet the pad surface, and fills out the interfacial cavities between the pads and the substrate (see Fig. 18). Similarly, secretion or mucus are used generally to enhance adhesion *e.g.*, in flies and tree frogs. The secretion fluid, observed in the footprints of many insects wets many hydrophilic as well as hydrophobic surfaces, such as wax or glass. It has been suggested that the fluid contains surfactants which would make adhesion less sensitive to the nature of the substrate.

In this context we note that the transfer of a high-viscosity, tacky, substance to the surface of the tires and to the road surface is exploited in race car tires. Thus, the rubber used for race car tires contains synthetic resins, which are high-viscosity tacky substances, similar to the sticky substance that oozes from fir and pine trees. This substance is transfered to the tire surface and to the road surface, and will fill out the small-sized cavities of the road surface (which the rubber itself would not be able to penetrate), and will hence increase the effective adhesion (and friction coefficient) between the surfaces. It is well known that the stickiness of the Formula 1 race tracks increases with time from the start of the race as a result of the continuous transfer of the sticky substance from tires to the race track.

14 Summary and conclusion

We have studied the influence of surface roughness on the adhesion of elastic solids. Most real surfaces have roughness on many different length scales, and this fact has been taken into account in our study. The theory allows for *partial* block-substrate contact on all length scales. We have considered in detail the case when the surface roughness can be described as self-affine fractal, and shown that when the fractal dimension $D_{\rm f} > 2.5$, the adhesion force may be strongly reduced. For surfaces with a fractal dimension close to 2, full contact occurs in the (apparent) contact areas except close to the long-distance cut-off length λ_0, where the contact may be only partial. For fractal dimension $D_{\rm f} > 2.5$ partial contact occurs on all length scales and the area of (apparent) contact decreases continuously with increasing magnification. We have studied the block-substrate pull-off force as a function of roughness. A particular important result is that even when the surface roughness is so high that no adhesion can be detected in a pull-off experiment, the area of real contact (when adhesion is included) may still be several times larger than when the adhesion is neglected. Since it is the area of real contact which determines the sliding friction force, it is clear that the adhesion interaction may strongly affect the friction force even when no adhesion can be detected in a pull-off experiment. The theory is in good qualitative agreement with experimental data. To test the theory quantitatively, we suggest that new experiments should be performed on surfaces for which the surface roughness power spectra have been measured.

I acknowledge a grant from BMBF related to the German-Israeli Project Cooperation "Novel Tribological Strategies from the Nano-to Meso-Scales." I also acknowledge EC for a "Smart QuasiCrystals" grant under the EC Program "Promoting Competitive and Sustainable GROWTH".

References

1. B.N.J. Persson, *Sliding Friction: Physical Principles and Applications*, second edition (Springer, Heidelberg, 2000).
2. J.N. Israelachvili, *Intermolecular and Surface Forces* (Academic Press, London, 1995).
3. B.N.J. Persson, Phys. Rev. Lett. **87**, 1161 (2001); J. Chem. Phys. **115**, 3840 (2001). See also B.N.J. Persson,

F. Bucher, B. Chiaia, to be published in Phys. Rev. B **65**, 184106 (2002).
4. K.N.G. Fuller, D. Tabor, Proc. R. Soc. London, Ser. A **345**, 327 (1975).
5. G.A.D. Briggs, B.J. Briscoe, J. Phys. D **10**, 2453 (1977).
6. K.N.G. Fuller, A.D. Roberts, J. Phys. D **14**, 221 (1981).
7. K. Kendall, *Molecular Adhesion and its Applications* (Kluwer, New York, 2001); D. Maugis, *Contact, Adhesion and Rupture of Elastic Solids* (Springer, Berlin, 1999).
8. A.N. Gent, R.P. Petrich, Proc. R. Soc. London, Ser. A **310** 433 (1969); M. Barquins, B. Khandani, D. Maugis, C. R. Acad. Sci. Paris, Ser. II, **303**, 1517 (1986); C. Derail, A. Allal, G. Marin, Ph. Tordjeman, J. Adhes. **61**, 123 (1997); L. Benyahia, C. Verdier, J.-M. Piau, J. Adhes. **62**, 45 (1997); A. Chiche, P. Pareige, C. Creton, C. R. Acad. Sci. Paris, Ser. IV, 1197 (2000); P. Tordjeman, E. Papon, J.-J. Villenave, J. Chem. Phys. **113**, 10712 (2000); C. Gay, L. Leibler, Phys. Rev. Lett. **82**, 936 (1999); A. Zosel, J. Adhes. **34**, 201 (1991). H. Lakrout, P. Sergot, C. Creton, J. Adhes. **69**, 307 (1999).
9. K.L. Johnson, K. Kendall, A.D. Roberts, Proc. R. Soc. London, Ser. A **324**, 301 (1971).
10. B.N.J. Persson, E. Tosatti, J. Chem. Phys. **115** 5597 (2001).
11. S. Zilberman, B.N.J. Persson, to be published in Solid State Commun.
12. K.L. Johnson, *Contact Mechanics* (Cambridge University Press, Cambridge, 1985).
13. J. Feder, *Fractals* (Plenum Press, New York, 1988).
14. M. Klüppel, G. Heinrich, Rubber Chem. Technol. **73**, 578 (2000).
15. M.V. Berry, Z.V. Lewis, Proc. R. Soc. London, Ser. A **370**, 459 (1980).
16. T.R. Thomas, *Rough Surfaces*, second edition (Imperial College Press, London, 1999)
17. G. Sperling, PhD Thesis, Karlsruhe Technical University (1964).
18. K. Kendall, J. Phys. D **4**, 1186 (1971); **6**, 1782 (1973); **8**, 115 (1975). See also the beautiful review article of K. Kendall, Contemp. Phys. **21**, 277 (1980).
19. B.V. Derjaguin, Wear **128**, 19 (1988); D. Tabor, in *Surface Physics of Materials*, Vol. **II**, edited by J.M. Blakely (Academic Press, New York, 1975) pp. 475-529.
20. See, *e.g.*, L.B. Freund, *Dynamics Fracture Mechanics* (Cambridge University Press, New York, 1990).
21. M. Scherge, S. Gorb, *Bilological Micro and Nano Tribology: Nature's Solutions* (Springer, Berlin, 2001).
22. A.L. Barabasi, H.E. Stanley, *Fractal Concepts in Surface Growth* (Cambridge University Press, Cambridge, 1995).
23. M. Barquins, D. Maugis, J. Adhes. **13**, 53 (1981).
24. M. Deruelle *et al.*, J. Adhes. Sci. Technol. **12**, 225 (1998).